Performance Analysis of IEEE 802.15.4 Beacon-Enabled Mode

Chiara Buratti
WiLAB, DEIS at University of Bologna, ITALY.
Email: c.buratti@unibo.it

***Abstract*—[1] In this paper a mathematical model for the beacon-enabled mode of the IEEE 802.15.4 Medium Access Control (MAC) protocol is provided. A Personal Area Network (PAN) composed of multiple nodes, which transmit data to a PAN coordinator through direct links or multiple hops, is considered. The application is query-based: upon reception of the beacon transmitted by the PAN coordinator, each node tries to transmit its packet using the superframe structure defined by the IEEE 802.15.4. Those nodes that do not succeed in accessing the channel, discard the packet; at the next superframe a new packet is generated. The aim of the paper is to develop a flexible mathematical tool able to study beacon-enabled 802.15.4 networks organized in different topologies. Both the Contention Access Period (CAP) and the Contention Free Period defined by the standard, are considered. The slotted Carrier Sense Multiple Access with Collision Avoidance algorithm used in the CAP portion of the superframe, is analytically modelled. The model describes the probability of packet successful reception and access delay statistics. Moreover both star and tree-based topologies are considered: suitable comparison between these topologies is provided. The model is a useful tool for the design of MAC parameters and for the choice of the topology. The mathematical model is validated through simulation results. The model differs from those previously published by other authors in the literature as it precisely follows the MAC procedure defined by the standard, in the context of the application scenario described above.**

***Index Terms*—IEEE 802.15.4, MAC, CSMA/CA, GTS, tree-based topology, Zigbee.**

I. Introduction

IEEE 802.15.4 [1], [2] is a short-range wireless technology intended to provide applications with relaxed throughput and latency requirements in wireless Personal Area Networks (PANs). The key features of 802.15.4 are low complexity, low cost, low power consumption, and low data rate transmissions.

In this paper, we consider a PAN composed of multiple devices (hereafter denoted as nodes), that have to transmit data to the PAN coordinator through single or multiple hops. We assume that the application requires periodic data at the PAN coordinator: each node upon reception of a query coming from the PAN coordinator, generates a packet and attempts to access the channel in order to transmit it. Therefore, each node has only one packet per query to be transmitted. If the node does not succeed in accessing the channel before the reception of the next query, the packet is lost and a new one is generated.

Examples of application of this scenario to realistic cases, can be easily found, for example, in the context of body area networks [3], [4] or wireless sensor networks (WSNs) [5]–[7]. 802.15.4, in fact, is one of the most suitable technologies for WSNs. In most of WSN applications, nodes are distributed over an environment with the aim of estimating a spatial process [5], like temperature or pressure: nodes periodically take samples of the process from the environment, to transmit it toward a data collector (that is the PAN coordinator in our scenario).

Both star and tree-based topologies are accounted for. In particular, first we deal with a star topology, that could be used when the number of nodes in the network is small (however, for the sake of validation of the model, also results for larger networks are shown). Then, a tree rooted at the PAN coordinator, is studied.

No connectivity issues are considered in this paper: in the star topology case it is assumed that all nodes can reach the coordinator, whereas in the tree-based topology case we assume that the children of a given parent may reach the parent itself.

The 802.15.4 standard allows two types of channel access mechanisms: beacon (this option is mandatory when tree topologies are used) or non beacon-enabled. The latter case uses unslotted Carrier Sense Multiple Access with Collision Avoidance (CSMA/CA), whereas in the former a slotted CSMA/CA algorithm and a superframe structure managed by the PAN coordinator, is used. As will be described in the following, the superframe starts with a packet transmitted by the PAN coordinator, denoted as beacon, and could include some slots allocated to given nodes, called Guaranteed Time Slots (GTSs).

Since periodic data acquisition at the PAN coordinator is required, the beacon-enabled mode is used; therefore, the beacon packet will coincide with the query.

Given the scenario described above, the scope of the paper is to provide a mathematical model for the description of the probability of packet successful reception and access delay statistics.

To such aim, the transitions between node states (backoff, sensing, transmit, idle) of the slotted CSMA/CA 802.15.4 Medium Access Control (MAC) protocol, have to be modelled. The probabilities of channel access and successful transmission are evaluated as a function of time, starting from reception of the beacon sent by the coordinator, till the end of the superframe. The model also allows the evaluation of the

overall success probability for a packet to be transmitted, the throughput, that is the number of bytes per unit of time successfully received by the coordinator, and the average delays. Performance is evaluated by changing the number of nodes, the duration of the superframe, the number of GTSs and the packet size. To validate the mathematical model, comparison to simulations is performed, and results show almost perfect match. Performance metrics are first evaluated for the star topology case, then the model is applied to a three-level tree-based topology and suitable comparison between the two topologies is also shown. Extension to the case of tree of any height is trivial.

The paper is outlined as follows: an overview of the literature is provided in Section II, Section III describes the IEEE 802.15.4 MAC protocol, Section IV deals with the scenario and the model assumptions. Section V introduces the metrics derived from the model, whereas in the Sections VI and VII the mathematical model of the slotted CSMA/CA algorithm and the related performance metrics are derived. Sections V, VI and VII are related to the star topology. The tree-based topology is discussed in Section VIII and numerical results for both the topologies are shown in Section IX. Finally, conclusions are reported in Section X. Part of the analytical formulation is left to Appendix A.

II. Related Works

In the literature, there exist several works devoted to the study of 802.15.4 networks. Performance evaluation of the 802.15.4 MAC protocol has been carried out by means of simulations [8]–[10]. Also some studies have tried to describe analytically the behavior of the 802.15.4 MAC protocol, as this paper does. However, none of them captures the exact essence of the IEEE 802.15.4 MAC in the scenario described here.

The model described in [11] fails to match simulation results, as described in [12], as the authors use the same Markov formulation and assumptions made by Bianchi in [13], where the 802.11 MAC protocol is considered. This protocol, in fact, is significantly different from the one defined by the 802.15.4 standard [14]. A better model is proposed in [15], where however, the probabilities of being in sensing in the two subsequent slots are not correctly captured by the Markov chain (see also [12]). In [16] the events of finding the channel free in the first and in the second slots are considered independent and the probabilities that those two events happen are assumed to be equal. As will be clarified in the following, instead, these events are not independent and this approximation causes notable differences between simulations and analytical results. An other model is presented in [17] where, however, different simplifying assumptions are made: the uniform distribution of the backoff counter within the backoff windows are assumed to be geometrically distributed, so that the backoff algorithm becomes memoryless. The model developed in [17] has been validated through simulations, only for a very small set of parameters, and only a network composed of 12 nodes is considered.

However, all the above cited works (also [12] and [17], which seem to provide the better models) are based on the Bianchi's model and use a Markov chain to describe node states even if the process representing the backoff time counter is not Markovian, since the value of the backoff counter depends on the past history (i.e., how many times the node has tried to access the channel and found it busy). To use a Markov chain, in fact, Bianchi assumes that at each transmission attempt and regardless of the number of retransmissions suffered (backoff stages in the 802.15.4 case), each packet collides with constant and independent probability (see [13]). This assumption results more accurate as long as the contention window and the number of nodes accessing the channel get larger. This approximation is good for the above mentioned works, being the number of nodes competing for the channel constant in time; however it is not accurate for query-based applications. In the scenario considered here, in fact, the number of nodes accessing the channel decreases by passing time (since nodes have only one packet to be transmitted per superframe upon reception of the query), resulting in a decreasing of the probability that a packet collides. The difference of the scenarios studied here and in the previous works, in fact, completely changes the form of the analysis. In the previous works, it is assumed that nodes have always [12], [13], [15], or with a certain probability [11], [18]–[20] a packet to be transmitted (in [17] Poisson distributed arrivals of packets is assumed). This means that once a node transmits its packet, it will start again the backoff algorithm, possibly with a certain probability which is known. In our model, instead, the number of nodes competing for channel access decreases with time. Therefore, according to the different scenario studied, the above mentioned assumption is removed and the probabilities (of being in sensing, transmission and of colliding) are evaluated for the different backoff stages and the different instants of time.

Moreover, one of the most important aims of this paper is to derive the access delay statistics. Since all the works cited [11]–[13], [15]–[17] studied the asymptotic behavior of the network at the equilibrium conditions, evaluating the stationary probabilities obtained when time tends to infinite, the statistics of traffic cannot be derived from these analyse.

Finally, it is worth noting that the works present in the literature do not analytically account for the modelling of GTSs, the duration of the superframe (that strongly affects performance, as shown in this paper) and tree-based topologies. All these issues, instead, are considered in this paper.

This paper is based on previous works [14], [21], where the non beacon-enabled mode is analysed. Even though the rationale used to derive the metrics is similar, the presence of the two subsequent sensing phases, characterising the slotted CSMA/CA of the beacon-enabled mode, significantly changes the model with respect to [14], [21]: a different finite state transmission diagram for modelling nodes states is needed and also the formulas for deriving the sensing and transmission probabilities are different. Moreover, in the beacon-enabled mode, the events of being in sensing in the two different phases and to find the channel free are not independent (as will be clear in the following, a node enters in the second sensing phase only in case it finds the channel free in the first

phase). This dependence makes the model developed here very different and more complex than the one developed in [14], [21]. In addition, in this model also the presence of GTSs and of a superframe having a given duration is taken into account. Finally, here tree-based topologies are studied, whereas in [14], [21] only star topologies are considered since the non beacon-enabled mode does not allow the formation of trees.

III. The IEEE 802.15.4 MAC protocol

According to the IEEE 802.15.4 MAC protocol in beacon-enabled mode [1], the access to the channel is managed through a superfrarme, starting with the beacon packet, transmitted by the PAN coordinator. The superframe is subdivided into three parts: an inactive part, a Contention Access Period (CAP), during which nodes use a slotted CSMA/CA, and a Contention Free Period (CFP), containing a number of GTSs, that can be allocated by the PAN coordinator to specific nodes. The PAN coordinator may allocate up to seven GTSs, but a sufficient portion of the CAP must remain for contention-based access. The minimum CAP duration is equal to 440 T_s, where T_s is the symbol time. Here we consider the 2.45 GHz band, meaning a symbol rate of 62.5 ksymbol/sec, which brings to have $T_s = 16\ \mu sec$ [1].

The duration of the active part and of the whole superframe, depend on the value of two integer parameters both ranging from 0 to 14: the superframe order, denoted as SO, and the beacon order, denoted as BO, being $BO \geq SO$. The latter, defines the interval of time between two successive beacons, namely the beacon interval, denoted as T_B given by: $T_B = 960 \cdot 2^{BO} \cdot T_s$. The duration of the active part of the superframe, containing CAP and CFP, namely the superframe duration, denoted as T_A, is given by: $T_A = 960 \cdot 2^{SO} \cdot T_s$.

The inactive part (present when $BO > SO$) is used for saving energy (nodes can switch off during this phase) or for exploiting multi-hop. Since the evaluation of energy consumption is out of scope of this paper, we set $SO = BO$ (i.e., $T_B = T_A$) in case of star topologies (one hop) and $BO > SO$ for trees. A proper setting of the parameters BO and SO in the latter case is needed: Section IX-B tries to provide some guidelines for this setting.

The CSMA/CA algorithm used in the CAP portion of the superframe is implemented using units of time called backoff periods: a backoff period has a duration, denoted as d_{bo}, equal to 20 T_s (320 μsec). The backoff period boundaries of every node in the PAN must be aligned with the superframe slot boundaries of the coordinator, therefore, the beginning of the first backoff period of each node is aligned with the beginning of the beacon transmission. Moreover, all transmissions may start on the boundary of a backoff period.

Each node maintains three variables for each transmission attempt: NB, CW and BE. NB is the number of times the CSMA/CA algorithm was required to backoff while attempting the current transmission. CW is the number of backoff periods that need to be clear of channel activity before the transmission can start. BE is the backoff exponent related to the maximum number of backoff periods a node will wait before attempting to assess the channel.

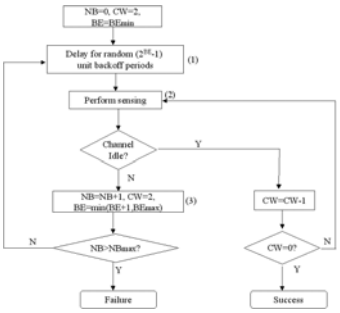

Fig. 1. The IEEE 802.15.4 CSMA/CA algorithm.

The algorithm follows the following steps (see Figure 1). First, NB, CW, and BE are initialized to 0, 2, and BE_{min}, respectively. Upon reception of the beacon, any activity is delayed (backoff state) for a random number of backoff periods in the range (0, $2^{BE} - 1$) [step (1)]. After this delay, channel sensing is performed for one backoff period [step (2)]. If the channel is assessed to be busy, CW is set to 2 and NB and BE are increased by 1, ensuring that BE is not larger than BE_{max}. If the value of NB is lower than NB_{max}, the algorithm returns to step (1); otherwise the algorithm will unsuccessfully terminate, meaning that the node does not succeed in accessing the channel. If the channel is assessed to be idle, instead, CW is decremented by 1 and compared with 0. If $CW > 0$, the algorithm returns to step (2); otherwise a transmission may start.

IV. The Reference Scenario and Model Assumptions

We consider a PAN composed of N nodes transmitting packets, having size, z, equal to $D \cdot 10$ bytes, being D an integer in the range [2,13], according to the minimum and maximum possible data packet size [1]. By assuming a 16-bit short address is used, the data frame has a size of $(6+11+n)$ bytes, where n is the size of the payload in bytes, 6 and 11 bytes are the physical and MAC overheads [1]. Therefore, in the case $D = 2$, we will have $n = 4$ bytes, and being the maximum packet size equal to 133 bytes, the maximum value of D is 13. The time needed to transmit a packet will be equal to $D \cdot d_{bo}$, as a bit rate of 250 kbit/sec is used; therefore, each packet occupies D backoff periods.

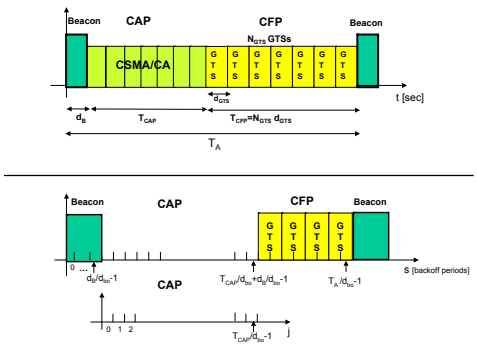

Fig. 2. The IEEE 802.15.4 superframe, considering the time axis (above part), and the number of slots, s, (below part).

We also denote as N_{GTS} the number of GTSs allocated (see Figure 2 above part). Therefore, in each superframe, N_{GTS} nodes will have a GTS allocated and will use the CFP to transmit their packets and the remaining $N - N_{GTS}$ nodes will use the CAP portion.

According to the standard each GTS must have a duration multiple of $60 \cdot 2^{SO} \cdot T_s$; we denote this duration as d_{GTS}, equal to $D_{GTS} \cdot 60 \cdot 2^{SO} \cdot T_s$, with D_{GTS} integer (see Figure 2, above part). Since an inter-frame space, between two successive packets received by the coordinator must be guaranteed, D_{GTS} is such that the GTS contains the packet and the inter-frame space. The inter-frame space duration depends on the size of the MAC protocol data unit (MPDU): for MPDU lower than 18 bytes an inter-frame space of 12 T_s must be present, whereas 40 T_s are needed for MPDU larger than 18 bytes [1]. We set the GTS duration equal to the minimum possible duration which allows to contain the packet and the inter-frame space. Therefore, by denoting as d_{ifs} the duration of the inter-frame space, we have $D_{GTS} = \lceil (D \cdot d_{bo} + d_{ifs})/(60 \cdot 2^{SO} T_s) \rceil$, and the number of backoff periods occupied by each GTS is equal to $D_{GTS} \cdot 3 \cdot 2^{SO}$.

Finally, we denote the beacon size as z_B and as d_B the instant in which the CAP starts (see Figure 2). Since alignment between the first backoff period of each node and the beginning of the beacon transmission is required, d_B will be equal to the beacon transmission time only in case it is multiple of d_{bo}, otherwise, it will be larger.

No hidden terminal problem is accounted for: all nodes competing for the channel can "hear" each other [11]–[13], [15]. The number of nodes competing for the channel that must be audible one to each other is the number of nodes in the network in the star topology case and the children of a given parent in the tree case (see Section VIII). In these conditions collisions may occur only in case two or more nodes perform channel sensing at the same time, find the channel free and transmit simultaneously their packets. For the sake of energy efficiency, no acknowledge and retransmission mechanism is implemented.

Having fixed the origin of time axis at the beginning of the superframe ($t = 0$) and all nodes will start the CSMA/CA algorithm at $t = d_B$, since no propagation delay is assumed due to short distances. As stated in Section I, we assume that in case a node does not succeed in accessing the channel by the end of the superframe, the packet is lost. According to our application scenario, in fact, it is reasonable to assume that once a node receives a new query it takes a new sample from the environment instead of trying to transmit the old one.

In the model, the resolution time (hereafter denoted as slot) is set equal to the backoff period, d_{bo}, which corresponds also to the duration of the single sensing phase and to the packet transmission time in the (ideal) case $D = 1$.

Therefore, since one of the aims of the model is to derive the statistics of the traffic generated by nodes in the whole superframe, we will study the behavior of the network in each slot. In the following we will denote as s, the s-th slot in the superframe, being $s \in [0, T_A/d_{bo} - 1]$.

V. Performance Metrics Derived from the Model

The model provides the following metrics:

- the probability that a node ends the transmission of its packet in a given slot s, denoted as $P\{T^s\}$, with $s \in [0, T_A/d_{bo} - 1]$;
- the probability that the coordinator receives the packet tail, coming from a node, in a given slot s, denoted as $P\{Z^s\}$, with $s \in [0, T_A/d_{bo} - 1]$;
- the success probability for a transmission, that is the probability that a node succeeds in transmitting its packet in the superframe whatever the slot, denoted as p_s;
- the average delay, D_{mean}, with which a packet is received by the coordinator.

We assume that when N_{GTS} GTSs are allocated, the coordinator randomly selects the N_{GTS} nodes to which allocate them. Therefore, no resource allocation strategies are accounted for. For the scenario considered, this assumption is reasonable, since all nodes transmit packets of the same size and no priority policy between nodes is needed. We also recall here that each node has only a packet to be transmitted per superframe, therefore it will use the CAP or the CFP (but not both). In these conditions, the probability that a node has a specific GTS allocated is $1/N$, whereas the probability that a node has whatever a GTS allocated (that is the probability that the node may use the CFP) is equal to N_{GTS}/N. However note that the model could be applied to whatever a GTS allocation strategy, by simply changing the probability $1/N$.

To simplify the formulas in the following, we will indicate with the integer j the slots in the CAP portion, and with $P\{T^j\}_{CAP}$ and $P\{Z^j\}_{CAP}$, the probabilities that a node succeeds in accessing the channel and in transmitting its packet in slot j of the CAP portion, being $j \in [0, T_{CAP}/d_{bo} - 1]$, where T_{CAP} is the duration of the CAP portion given by: $T_{CAP} = T_A - d_B - N_{GTS} \cdot d_{GTS}$. Therefore, we simply set $j = s - d_B/d_{bo}$ (see Figure 2).

Therefore, the probabilities $P\{T^s\}$ and $P\{Z^s\}$ in the CAP portion are given by:

$$P\{T^s\} = P\{T^j\}_{CAP} \cdot \frac{N - N_{GTS}}{N} 1\,, \tag{1}$$

for $s \in [d_B/d_{bo}, T_{CAP}/d_{bo} + d_B/d_{bo} - 1]$ and $j \in [0, T_{CAP}/d_{bo} - 1]$; and null otherwise.

$$P\{Z^s\} = P\{Z^j\}_{CAP} \cdot \frac{N - N_{GTS}}{N}\,, \tag{2}$$

for $s \in [d_B/d_{bo}, T_{CAP}/d_{bo} + d_B/d_{bo} - 1]$ and $j \in [0, T_{CAP}/d_{bo} - 1]$; and null otherwise.

In the CFP, $P\{T^s\} = P\{Z^s\} = 1/N$ for $s = T_{CAP}/d_{bo} + d_B/d_{bo} + k \cdot D_{GTS} \cdot 3 \cdot 2^{SO} + D - 1$, with $k \in [0, N_{GTS} - 1]$; and null otherwise. Recall that transmissions are referred to the last slot in which the transmission occurs and that no collisions happen in GTSs.

We can also evaluate the cumulative functions, $F_T(s)$ and $F_Z(s)$, defined as the probability that a node transmits its packet within slot s, and that a node transmits correctly its packet within s, respectively, given by: $F_T(s) = \sum_{v=0}^{s} P\{T^v\}$, and $F_Z(s) = \sum_{v=0}^{s} P\{Z^v\}$.

The success probability, p_s, for a packet transmitted by a node in a network composed of N nodes organised in a star topology is:

$$p_s(N) = p_{s_{CAP}}(N - N_{GTS}) \cdot \frac{N - N_{GTS}}{N} + \frac{N_{GTS}}{N}, \quad (3)$$

where $p_{s_{CAP}}(N - N_{GTS})$ is the success probability for a packet transmitted in the CAP portion, through the CSMA/CA algorithm, when $N - N_{GTS}$ nodes compete for the channel. The success probability for a packet transmitted in the CFP, instead, is equal to one.

Finally the average delay, D_{mean}, is given by:

$$D_{mean} = d_{bo} \cdot \sum_{s=0}^{T_A/d_{bo}-1} (s+1)\frac{P\{Z^s\}}{p_s}, \quad (4)$$

where $s + 1$ is the delay, in backoff periods, of a packet correctly received in slot s, and $\frac{P\{Z^s\}}{p_s}$ is the probability that the packet tail is received in slot s, given that the packet has been correctly received.

The probabilities $P\{T^j\}_{CAP}$, $P\{Z^j\}_{CAP}$ and $p_{s_{CAP}}$, related to the CAP portion are derived in the following Sections where the mathematical model of the CSMA/CA algorithm is introduced.

For the sake of clarity, the list of variables used in the paper is provided in Table I.

TABLE I
VARIABLES DEFINITION.

N	Number of nodes in the network
N_{GTS}	Number of GTSs allocated
T_B	Beacon Interval
T_A	Superframe duration
T_s	Symbol time
T_{CAP}	CAP duration
d_B	Beacon duration
d_{GTS}	Duration of a GTS
d_{bo}	Backoff period duration
d_{ifs}	Inter-frame space duration
$P\{T^s\}$	Prob. a node ends tx in slot s
$P\{Z^s\}$	Prob. coord. rx packet tail in slot s
p_s	Success probability
$P\{T^j\}_{CAP}$	Prob. a node ends tx in slot j in the CAP
$P\{Z^j\}_{CAP}$	Prob. coord. rx packet tail in slot j in the CAP
$p_{s_{CAP}}$	Success probability in the CAP
b_w^j	Prob. to find the channel busy when $CW = w$, at slot j
f^j	Prob. to find the channel free in slots $j-1$ and j
D	Number of backoff periods occupied by a packet
S	Throughput
G	Offered traffic
D_{mean}	Average delay
z	Data packet size
z_B	Beacon packet size

VI. FORMULATION OF THE MATHEMATICAL MODEL FOR THE CAP

A. Node States

Generally speaking, a node accessing the channel during the CAP portion of the superframe can be in one of four states: backoff, sensing, transmission, or idle. However, if after sensing the channel is free for two subsequent slots, transmission immediately occurs, followed by a sequence of idle states till the end of the superframe. Thus, given the objectives of this paper, we need to model only the backoff and sensing states.

The node state is modeled as a three-dimensional process $Q(\hat{t})$=$\{BO_c(\hat{t}), BO_s(\hat{t}), CW(\hat{t})\}$, where $\hat{t}$ is an integer, representing the time, expressed in number of slots, having set the origin of this time axis ($\hat{t} = 0$) at the instant in which nodes receive the beacon. Therefore, $\hat{t} = j$ denotes the j-th slot (from $j \cdot d_{bo}$ to $(j + 1) \cdot d_{bo}$), after the reception of the beacon, that is the interval of time between $d_B + j \cdot d_{bo}$ and $d_B + (j + 1) \cdot d_{bo}$.

$BO_c(\hat{t})$ and $BO_s(\hat{t})$ represent the backoff time counter and the backoff stage at time $\hat{t}$, respectively, and $CW(\hat{t})$ is the value of CW at time $\hat{t}$. $BO_c(\hat{t})$ counts the number of slots a node must wait before sensing the channel; whereas $BO_s(\hat{t})$ dimensions the maximum duration of the backoff phase. $BO_c(\hat{t})$ and $BO_s(\hat{t})$ are time-discrete stochastic processes assuming discrete values. Therefore, the process is a chain; however, it is not a Markovian chain [22] because $BO_c(\hat{t})$ is not a memoryless process as its value depends on its history.

The initial value of backoff time counter ($BO_c(0)$) is uniformly distributed in the range [0, $W_{NB} - 1$], where $W_{NB} = 2^{BE}$ is the dimension of the contention window and $NB \in [0, NB_{max}]$. The value of BE depends on the second process characterizing the state: $BO_s(t)$. We can identify $NB_{max} + 1$ different backoff stages obtained by considering the different possible combinations of the pair (NB, BE). In Table II, the different backoff stages with the correspondent W_{NB} values (denoted as W_0 ,.., $W_{NB_{max}}$) are shown.

The 802.15.4 MAC protocol states that at the beginning of the backoff algorithm, each node sets $NB = 0$ and $BE = BE_{min}$. Then, each time the channel is sensed busy, NB and BE are increased by 1. When BE reaches its maximum value, there is no more increase. The case $BO_s = NB_{max}$ is the last case, because here NB reaches its maximum value, and it cannot be further increased.

Since there exists a maximum value for NB, there will be also a maximum delay affecting the transmission of a packet. This maximum is reached in case a node extracts at every backoff stage the higher backoff time counter and at the end of each backoff stage it always finds the channel busy. Therefore, the last slot in which a transmission can start is $\hat{t}_{max} = \sum_{k=0}^{NB_{max}} W_k + k + 1$, and the last slot in which a transmission can finish is $(\hat{t}_{max} + D - 1)$.

In the following, the generic state will be denoted as $Q(\hat{t})$=$\{BO_c, BO_s, CW, \hat{t}\}$ and the probability of being in a generic state will be denoted as $P\{BO_c$=c, BO_s=i, CW=$w, \hat{t}$=$j\}$=$P\{c, i, w, j\}$. In particular, the probability of being in a backoff state, will be denoted as $P\{c, i, 2, j\}$, since in these states CW is equal to 2. Whereas the probability of being in the first sensing phase (i.e., when $CW = 2$) and in the second sensing phase (i.e., when $CW = 1$) at the j-th slot and in the i-th backoff stage, will be denoted as $P\{S2_i^j\}$=$P\{0, i, 2, j\}$ and $P\{S1_i^j\}$=$P\{0, i, 1, j\}$, respectively. Note that when a node is in sensing BO_c is

equal to zero.

TABLE II
THE BACKOFF STAGES.

BO_s	NB	BE	$W_{NB} = 2^{BE}$
0	0	BE_{min}	$W_0 = 2^{BE_{min}}$
1	1	$BE_{min}+1$	$W_1 = 2^{BE_{min}+1}$
..	..	..	..
NB_{max}	NB_{max}	BE_{max}	$W_{NB_{max}} = 2^{BE_{max}}$

B. Steps Followed by the Model

Let us denote as b_w^j the probability that in the j-th slot when $CW = w$ the channel is found to be busy after sensing. Since CW is equal to 2 when a node performs the first sensing phase and to 1 when it performs the second sensing phase, we will denote as b_2^j the probability to find the channel busy in the first phase and as b_1^j the probability to find the channel busy in the second phase. Finally, we will denote as f^j, the joint probability to find the channel free in slot j and in slot $j-1$ (i.e., the probability that a node starting sensing in slot $j-1$ finds the channel free for two subsequent slots). These probabilities will be initially left as parameters, and their computation will be performed in Section VII-C. The model provides $P\{T^j\}_{CAP}$ and $P\{Z^j\}_{CAP}$, with $j \in [0, T_{CAP}/d_{bo} - 1]$, and $p_{s_{CAP}}$.

The probability $P\{T^j\}_{CAP}$ depends on the probability of being in sensing state in the slot $j - D - 1$ (since a packet occupies D slots) and to find the channel free for two subsequent slots. To determine the sensing probabilities, we model the behavior of a single node, using a state-transition diagram [22], describing the relation between all possible states in which a node can be (see below). From this diagram, we obtain the probabilities $P\{S1_i^j\}$ and $P\{S2_i^j\}$, whatever j and i are. This is made in the remainder of this Section. From these probabilities, we can derive the probabilities $P\{T^j\}_{CAP}$ (see Section VII-A). The probabilities $P\{Z^j\}_{CAP}$ and $p_{s_{CAP}}$, instead, are derived in Section VII-B. Section VII-C gives b_1^j, b_2^j and f^j.

C. Sensing Probabilities

The state-transition diagram of the three-dimensional process $Q(\hat{t})$ is presented through different Figures: one for each backoff stage. The part of the diagram related to the first backoff stage ($BO_s = 0$), obtained when the MAC parameters are set to the default values ($BE_{min} = 3$, $BE_{max} = 5$, $NB_{max} = 4$), is reported in Fig. 3 and commented in this Section. The part of the diagram related to the generic backoff stage ($BO_s = k$) is, instead, reported in the Figs. 13, 14 and commented in Appendix A.

As will be clarified in the following, the different Figures are linked together through transitions that originate from some states of a Figure and terminate in the states of the Figure related to the following backoff stage. Because each Figure is related to a specific value of BO_s, for the sake of simplicity in the drawings, the generic backoff state (ovals in the Figures) is simply denoted as $\{c, j\}$, omitting the value of BO_s, and also the value of CW, equal to 2 for all the backoff states. The sensing states (squares) are denoted as $S1^j$ and $S2^j$ with no pedex i. Finally the transmission states (triangles in the Figures) are denoted as T^j, with no pedex i.

In the following the part of the diagram related to the first backoff stage is described. The probabilities of being in the different states of the chain and the transition probabilities between the states are provided.

At the beginning of the backoff algorithm, each node extracts an integer, uniformly distributed between 0 and $W_0 - 1$. At $\hat{t} = 0$ a node enters, with probability $1/W_0$, one of the states $\{c, 0, 2, 0\}$ with $c \in [0, W_0 - 1]$. If the extracted value is 0, the node in slot 0 and 1 will sense the channel and in slot 2 it will transmit its packet, because no transmission may occur in the first two slots and, therefore, the channel will be certainly found free ($f^1 = 1$). In case a value larger than 0 is extracted, the node will decrease its backoff counter at each slot until the counter will reach the zero value, when the node will start sensing. In case the channel is found free for two subsequent slots the node will transmit the packet; otherwise it will pass to the following backoff stage and another value, uniformly distributed between 0 and $W_1 - 1$, will be extracted. In Figure 3, the transitions that originated from the sensing states enter in the states of part of the diagram related to $BO_s = 1$, shown in Fig. 13 once we set $k = 1$. For example, if a node is in the state $S2_0^1$ and it finds the channel busy, it will enter the state $S2_1^2$, or one of the states $\{c, 1, 2, 2\}$, with $c \in [1, W_1 - 1]$, with the same probability b_2^1/W_1. The state of arrival depends on the new backoff counter value extracted.

Denoting as $P\{BO_c = c_1, BO_s = i_1, CW = w_1, \hat{t} = j_1 | BO_c = c_0, BO_s = i_0, CW = w_0, \hat{t} = j_0\}$=$P\{c_1, i_1, w_1, j_1 | c_0, i_0, w_0, j_0\}$, the transition probability from the state $\{c_0, i_0, w_0, j_0\}$ to the state $\{c_1, i_1, w_1, j_1\}$, the transition probabilities between the backoff states are given by:

$$P\{c, 0, 2, j+1 | c+1, 0, 2, j\} = 1 \ , \tag{5}$$

for $c \in [0, W_0 - 2]$ and $j \in [0, W_0 - 2]$. This equation accounts for the fact that, at the beginning of each time slot, the backoff time counter is decreased by 1 until it reaches the zero value, with probability 1.

The probabilities of being in a sensing state when $CW = 2$ are given by:

$$P\{S2_0^j\} = \begin{cases} \frac{1}{W_0} & \text{for } j \in [0, W_0 - 1] \\ 0 & \text{otherwise .} \end{cases} \tag{6}$$

The probabilities of being in a sensing state when $CW = 1$ are given by:

$$P\{S1_0^j\} = \begin{cases} P\{S2_0^{j-1}\} \cdot (1 - b_2^{j-1}) & \text{for } j \in [1, W_0] \\ 0 & \text{otherwise .} \end{cases} \tag{7}$$

A node, in fact, will sense the channel for the second time if and only if it finds the channel free during the first sensing phase.

Similar formulas are achieved for the other backoff stages and are reported in Appendix A.

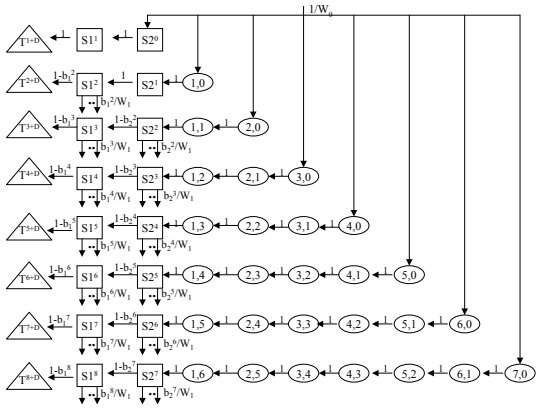

Fig. 3. The state-transition diagram of the first backoff stage.

VII. Performance Evaluation for the CAP

A. Transmission Probabilities

As stated before, the aim of the model is to evaluate the probability that a generic node ends its packet transmission in slot j, $P\{T^j\}_{CAP}$, with $j \in [0, T_{CAP}/d_{bo} - 1]$.

A node finishes its transmission in slot j, if in slot $j-D-1$, it starts sensing the channel finding it free for two subsequent slots. The probability that a node starts sensing in slot j, is the sum of the probabilities of starting sensing in the j-th slot and at the i-th backoff stage, considering all the possible backoff stages. Therefore, we obtain:

$$P\{T^j\}_{CAP} = f^{j-D} \cdot \sum_{k=0}^{NB_{max}} P\{S2_k^{j-D-1}\} \qquad (8)$$

for $j \in [D+1, \hat{t}_{max} + D - 1]$, and null otherwise. Because a node transmits a packet occupying D slots, we associate $P\{T^j\}_{CAP}$ to the slot in which the transmission terminates.

Eq. (8) is substituted in eq. (1) to derive the statistics in the whole superframe.

B. Success Probability

To evaluate the other target probabilities, we have to model how the number of nodes that compete for the access to the channel varies with time. We denote as N_c^j the number of nodes which have not transmitted yet at the end of slot $j-1$ and that will compete for slot j. By passing time, some nodes in the network may access to the channel, therefore, the number of nodes competing for the channel, decreases by increasing j. In particular, as shown in [14], N_c^j is a random variable, binomially distributed. However a precise evaluation of the statistics of this variable is complex from the computational viewpoint, since it depends on the statistics of N_c^{j-1}, whose determination would depend on the statistics of N_c^{j-2} and so on. To reduce such complexity, in [14] different approximations have been introduced and results achieved through such approximations have been compared. Results show that these approximations bring approximatively to the same results, therefore here we use the simplest approximation, according to which we set $N_c^j = N_c$, whatever j is. In the case of star topologies, N_c is the number of nodes using the CAP, therefore $N - N_{GTS}$. In Section IX, simulations are compared with the mathematical approach. Results show that a very good agreement with simulations is obtained through the model, despite the approximation introduced.

The probability, $p_{s_{CAP}}$, that a generic packet is transmitted successfully on the channel given by:

$$p_{s_{CAP}} = \begin{cases} \sum_{j=0}^{\hat{t}_{max}+D-1} P\{Z^j\}_{CAP} \\ \qquad \text{if} \quad \hat{t}_{max} + D - 1 \le T_{CAP}/d_{bo} - 1 \\ \sum_{j=0}^{T_{CAP}/d_{bo}-1} P\{Z^j\}_{CAP} \qquad \text{otherwise}\,, \end{cases} \qquad (9)$$

where $P\{Z^j\}_{CAP}$ is the probability that a successful transmission ends in slot j, which means that one and only one transmission starts in $j - D + 1$.

As only one transmission starts in slot $j - D + 1$ if only one node, over N_c, senses the channel in slot $j-D$ and if the channel is free in $j - D$ and $j - D - 1$, $P\{Z^j\}_{CAP}$ is given by:

$$P\{Z^j\}_{CAP} = f^{j-D} \cdot \sum_{k=0}^{NB_{max}} P\{S2_k^{j-D-1}\} \cdot \cdot \prod_{k=0}^{NB_{max}} (1 - P\{S2_k^{j-D-1}\})^{N_c-1}\,, \qquad (10)$$

where the second factor gives the probability that one node senses the channel in $j - D - 1$, whatever the backoff stage, and the third factor gives the probability that the remaining $N_c - 1$ nodes do not sense the channel in slot $j - D - 1$.

C. Probability to find the channel busy

The channel will be found busy in slot j in case a transmission starts in slot j, or in slot $j - 1$, up to slot $j - D + 1$, since each node transmits a packet occupying D slots. Therefore, by denoting as $P\{T_1^j\}$ the probability that at least one transmission starts in slot j, the probability to find the channel busy during the first sensing phase ($CW = 2$) is given by:

$$b_2^j = \sum_{v=j-D+1}^{j} P\{T_1^v\}\,. \qquad (11)$$

Whereas, b_1^j is the probability to find the channel busy conditioned to the fact that the channel in $j - 1$ was free, since a node performs the second sensing phase only if it has found the channel free in the first slot. Therefore, it is the probability that slot $j - 2$ is free and that there is at least one node starting sensing in this slot:

$$b_1^j = (1 - b_2^{j-2}) \cdot \left[1 - \prod_{k=0}^{NB_{max}} (1 - P\{S2_k^{j-2}\})^{N_c-1}\right]\,, \qquad (12)$$

where the second factor (between the brackets), is the probability that at least one node starts sensing in slot $j - 2$.

The channel will be jointly free in slots j and $j - 1$ if no transmissions start in slot j, $j - 1$, up to $j - D$, therefore, the

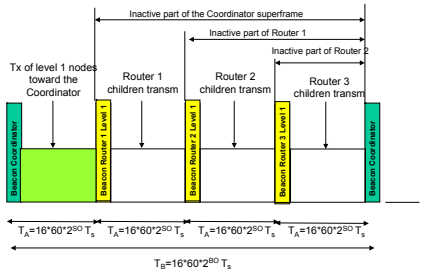

Fig. 4. The superframe structure used in the tree-based topology.

probability f^j is given by:

$$f^j = 1 - \sum_{v=j-D}^{j} P\{T_1^v\}\,. \tag{13}$$

Finally, the probability that at least one transmission starts in slot j is given by:

$$P\{T_1^j\} = f^{j-1} \cdot \left[1 - \prod_{k=0}^{NB_{max}} (1 - P\{S2_k^{j-2}\})^{N_c - 1}\right]. \tag{14}$$

VIII. The Tree-Based Topology

As stated above, when the number of nodes in the PAN gets larger, star topologies are not suitable and peer-to-peer or tree-based topologies should be used [2], [23]. An L-level tree, rooted at the PAN coordinator (namely, at level zero) is considered. Level i nodes receive data from level $i+1$ nodes and forward them to level $i-1$ nodes, toward the coordinator. The tree-based topology defined by the Zigbee Alliance [2] is accounted for.

According to the Zigbee specifications, the tree formation procedure is started by the PAN coordinator, which broadcasts beacons to nodes. A candidate node receiving the beacon may request to join the network at the coordinator. If the coordinator allows the node to join, it will start transmitting beacons to allow other candidate nodes joining the network.

Nodes work in beacon-enabled mode: each child node tracks the beacon of its parent and transmits its own beacon at a predefined offset with respect to the beginning of its parent beacon. The offset must always be larger than the parent superframe duration and smaller than beacon interval. This implies that the beacon and the active part of child superframe reside in the inactive period of the parent superframe: no overlap between the active portions of the superframes of child and parent is present (see Figure 4 as an example). This concept can be expanded to cover more than two nodes: the selected offset must not result in beacon collisions with neighbouring nodes. Obviously a child will transmit a beacon packet only in case it is a router. Each child will transmit its packet to the parent in the active part (CAP or CFP) of the parent superframe.

We set the duration of all the active parts of the superframes generated by the routers and by the coordinator at the same value (i.e., we set a unique value of SO). In these conditions, once we set the BO value, the number of routers (including the coordinator) that will have a portion of superframe available for receiving data from their children, will be equal to 2^{BO-SO} (see Figure 4). If the number of routers in the network is larger than 2^{BO-SO} some routers will not have a portion of superframe available, their children cannot access the channel and their packets will be lost. We denote as p_{frame_i} the probability that a level i router has a portion of superframe allocated, in which it can receive data from its children.

We denote as p_i the probability that a node is at level i of the hierarchy and with $p_s(n_i)$, the success probability for a level i node competing for the channel with the other $n_i - 1$ nodes, connected to the same parent at level $i-1$. A packet coming from a level i node will be correctly received by the coordinator, in case it is successfully transmitted by the level i node from which it is generated, and by all the routers from level $i-1$ till level one, forwarding it toward the coordinator. The success probability for a node accessing the channel in the tree is therefore:

$$p_{s_{tree}} = \sum_{i=1}^{L-1} p_i \cdot p_{frame_{i-1}} \cdot \prod_{k=1}^{i} \overline{p_{s_k}}\,. \tag{15}$$

where $\overline{p_{s_k}}$ is the average success probability for a node at level k, given by:

$$\overline{p_{s_k}} = \sum_{n_k=0}^{N_k} p_s(n_k) \cdot Prob\{n_k\} \tag{16}$$

where $Prob\{n_k\}$ is the probability to have n_k nodes at level k connected to the same parent at level $k-1$ and N_k is the total number of nodes at level k. According to the channel access strategy defined above, only the children of a given parent compete for the channel, therefore the tree could be seen as a series of stars, each having a parent and its children, operating independently (i.e., without collisions). Therefore, $p_s(n_k)$ is given by eq. (3), by simply setting $N = n_k$; whereas $Prob\{n_k\}$ depends on the strategy used to form the tree.

Note that equation (15) could be used to evaluate the success probability for a node accessing the channel when a L-level tree-based topology is established, whatever the strategy used to realise the tree.

Now the success probability $p_{s_{tree}}$ is evaluated in the particular case of a three-level tree ($L = 3$). We denote as $N_i = p_i \cdot N$, the number of level i nodes. We assume that each level one router performs data aggregation: the received packets are aggregated to that generated by the router itself, resulting in a packet of the same size of the single aggregated packets. We also assume that level two nodes select randomly the level one parent and that the active part of the coordinator superframe is used by level one nodes to transmit toward the PAN coordinator. The remaining $2^{BO-SO} - 1$ superframe portions are randomly allocated to level one routers for receiving data from their children. Under such assumption $p_{frame_0} = 1$, whereas there exists a certain probability, p_{frame_1}, that a level one router has not a portion of the superframe available. This probability is given by:

$$p_{frame_1} = \frac{2^{BO-SO}-1}{N_R}\,, \tag{17}$$

where N_R is the mean number of level one routers, that is the number of level one nodes with at least one child, given by:

$$N_R = \sum_{i=0}^{N_1} \binom{N_1}{i} (p_{child})^i \cdot (1-p_{child})^{N_1-i}\,. \tag{18}$$

Where $p_{child} = 1-(1-\frac{1}{N_1})^{N_2}$ is the probability that a level one node has at least a child, and $1/N_1$ is the probability that a level two node is connected to a given level one node.

Since level two nodes randomly select level one nodes to which transmit to, the number of level two nodes connected to the same level one node will be binomially distributed:

$$Prob\{n_2 = i\} = \binom{N_2}{i}\left(\frac{1}{N_1}\right)^i \cdot \left(1-\frac{1}{N_1}\right)^{N_2-i}\,. \tag{19}$$

Therefore, the average success probability for a node being at level two will be:

$$\overline{p_{s_2}} = \sum_{i=0}^{N_2} p_s(i) \cdot \binom{N_2}{i}\left(\frac{1}{N_1}\right)^i \cdot \left(1-\frac{1}{N_1}\right)^{N_2-i}\,, \tag{20}$$

where $p_s(i)$ is the success probability given by eq. (3) when i nodes at level two are competing for transmitting to the same level one node. Finally, according with eq. (15), we achieve

$$p_{s_{tree}} = p_1 \cdot \overline{p_{s_1}} + p_2 \cdot p_{frame_1} \cdot \overline{p_{s_1}} \cdot \overline{p_{s_2}}\,, \tag{21}$$

where p_{frame_1} is given by eq. (17), and $\overline{p_{s_1}} = p_s(N_1)$.

The average delay, denoted as $D_{mean_{tree}}$ in the case of tree, depends on the average delays of the packets coming from level one and level two nodes, denoted as D_{mean_1} and D_{mean_2}, respectively.

As stated above, level one nodes use the first portion of the superframe defined by the coordinator to transmit packets (see Fig. 4). Since these nodes could be seen as nodes of a star topology transmitting their packets directly to the coordinator, according to eq. (4), we obtain:

$$D_{mean_1} = d_{bo} \cdot \sum_{s=0}^{T_A/d_{bo}-1} (s+1)\frac{P\{Z^s\}(N_1)}{p_s(N_1)}\,, \tag{22}$$

where $\frac{P\{Z^s\}(N_1)}{p_s(N_1)}$ is the probability that the packet tail is correctly received by the coordinator in slot s, when N_1 nodes compete for the channel, given that the packet is correctly received. T_A is the duration of the active part of the superframe defined by the coordinator.

A packet coming from a level two node, instead, must be transmitted toward the level one parent and then from the latter to the coordinator. Therefore, two superframes are needed, one for each hop. Level one routers, in fact, always transmit to the coordinator the packets received by their children in the previous superframe. Therefore, the total average delay suffered by a level two node packet will be equal to T_B plus the average delay of its parent (i.e., the average delay of a level one node packet): $D_{mean_2} = D_{mean_1} + T_B$. Note that D_{mean_2} does not depend on the instant in which the parent receives the packet within its superframe.

Finally the average delay suffered by a packet coming from whatever a node in a tree is given by:

$$D_{mean_{tree}} = p_1 \cdot D_{mean_1} + p_2 \cdot D_{mean_2}\,. \tag{23}$$

IX. Numerical Results

A. The Star Topology

For the purpose of numerical comparison, a dedicated simulation tool written in C language, has been developed. The simulator generates a network composed of N nodes and a PAN coordinator, sending beacons and waiting for the data from nodes. In case GTSs are used, the PAN coordinator randomly selects the N_{GTS} nodes to which allocate GTSs, whereas the remaining nodes will use the CAP portion. According to the application scenario nodes has only one packet per superframe to be transmitted and, in case the CAP is used, they start the CSMA/CA algorithm at the same time. The CSMA/CA protocol described in Section III is implemented. Ideal channel conditions are assumed; therefore, all nodes can "hear" each other and can receive correctly the query at each round. No capture effect is considered: in case two or more packets collide, they are all lost. Finally, no acknowledge and retransmission mechanisms are performed. We consider 10^4 transmissions in our simulator, meaning that 10^4 queries and superframes are simulated.

In the following we set $d_{ifs} = 12\,T_s$ for the case $D = 2$, $d_{ifs} = 40\,T_s$ for the cases $D > 2$ and $z_B = 60$ bytes assuming that a payload is present in the beacon packet.

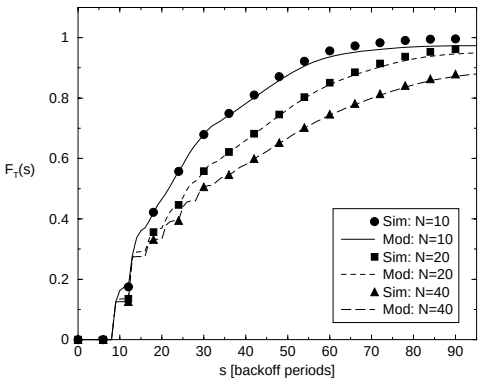

Fig. 5. The cumulative function, $F_T(s)$, when no GTSs are allocated, $D = 2$.

In Figures 5 and 6, the cumulative functions F_T, as a function of time, s, for different values of N, having set $D = 2$ when no GTSs and seven GTSs are allocated, are shown. Both mathematical (lines) and simulation (symbols) results are reported to validate the model: an excellent agreement between the two cases can be found in all cases. Results are obtained by setting $SO = 1$, therefore T_A=30.72 ms. No traffic toward the PAN coordinator in the first part of the superframe owing to the transmission of the beacon and to the sensing phases. As expected, by increasing N, the delay with which a node accesses the channel increases. The curves do not reach the

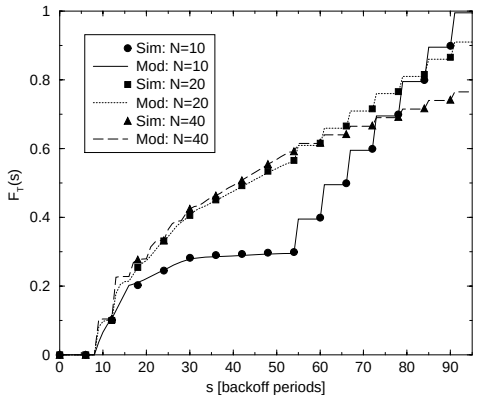

Fig. 6. The cumulative function, $F_T(s)$, when seven GTSs are allocated, $D = 2$.

value 1, since some nodes do not succeed in accessing the channel by the end of the superframe. The step-wise behavior of curves is motivated by the move from one backoff stage to the following. $P\{T^j\}_{CAP}$, in fact, present relative maxima at the beginning of each backoff window (i.e., the interval of time in which transmissions of nodes performing the first, the second, etc.. backoff stage, occur), whereas is approximately constant inside each backoff window [14].

In Figure 6 we can observe the statistics of the traffic in the CFP, characterised by steps in each GTS. Being $d_{ifs} = 12\,T_s$, we have $D_{GTS} = 1$. The reason why the curves in the CAP portion of the superframe are down scaled with respect to those of Fig. 5, is that here the traffic in the CAP is due to the presence of $N - N_{GTS}$ nodes instead of N. Moreover, nodes use the CAP only in case they do not have a GTS allocated (i.e., with probability $(N - N_{GTS})/N$). For these reasons the traffic in the CAP portion decreases.

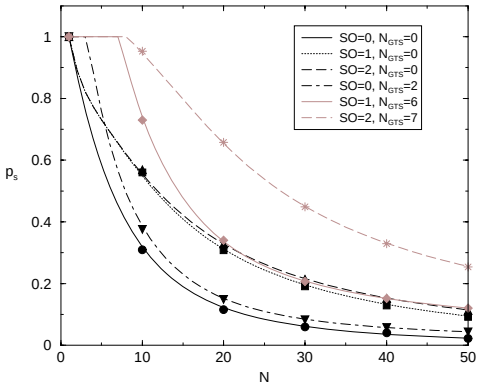

Fig. 7. The success probability, p_s as a function of N, $D = 5$.

In Figures 7 p_s as functions of N, for different values of SO, having fixed $D = 5$ is shown. The cases of no GTSs and N_{GTS} equal to the maximum number of GTSs allocable, are considered. As explained above, this maximum number depends on the values of D and SO. As we can see, p_s decreases monotonically (for $N > 1$ when $N_{GTS} = 0$ and for $N > N_{GTS}$ when $N_{GTS} > 0$), by increasing N, since the number of nodes competing for the channel increases. As expected the use of GTSs improves performance, since less nodes compete for the channel. By increasing SO, p_s gets larger, since the CAP duration increases and nodes have more time to access the channel.

Now we introduce the concepts of throughput, denoted as S, and offered traffic, denoted as G. We define the throughput as the number of bytes per unit of time successfully transmitted to the coordinator, and the offered traffic as the maximum number of bytes the network was deployed to deliver per unit of time. G is given by:

$$G = \frac{N \cdot z}{T_B}\,[bytes/sec]\,. \tag{24}$$

Whereas S is given by:

$$S = p_s \cdot G = \frac{N \cdot z}{T_B}\left(p_{s_{CAP}} \cdot \frac{N - N_{GTS}}{N} + \frac{N_{GTS}}{N}\right) = \\ = \frac{z}{T_B}\left[p_{s_{CAP}} \cdot (N - N_{GTS}) + N_{GTS}\right] \quad [bytes/sec]\,. \tag{25}$$

Have in mind that $z = D \cdot 10$ bytes and $T_B = T_A$ (since SO =

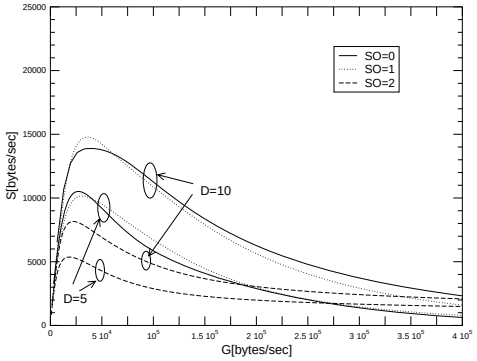

Fig. 8. The throughput S as a function of G, when no GTSs are allocated.

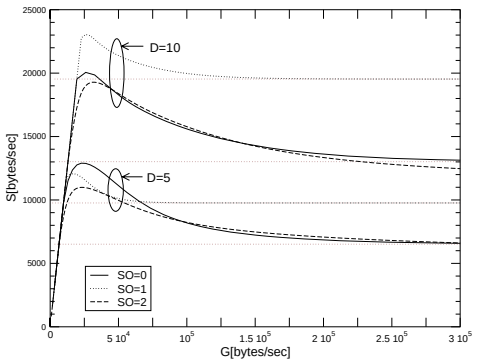

Fig. 9. The throughput S as a function of G, when the maximum number of GTSs is allocated.

In Figures 8 and 9, S as a function of G, when varying SO (i.e., T_A) and D, when no GTSs and when the maximum number of GTSs is allocated are shown, respectively. When few nodes are distributed in the network, by increasing G, S gets larger. With many nodes an increase of G results in a decrease of S, since many nodes are competing for the

channel. This means that in star topologies it is not convenient to increase too much N (i.e., the cost of the network), since many packets will be lost and also that when N gets larger star topologies are not suitable (this outcome was in fact expected). Moreover, we can note that there exists a value of SO maximising S, which depends on G and D. As an example, for $D = 5$ when G is small, an increase of SO even though p_s increases, results in a decrement of S, since S also depends on $1/T_A$. When, instead, the offered traffic gets larger, collisions increase and larger values of SO are required. On the other hand, when $D = 10$, the optimum value of SO is 1, for low G. This is due to the fact that, having large packets, when $SO = 0$ too many packets are lost, owing to the short duration of the superframe.

When no GTSs are allocated (Figure 8) S decreases monotonically since $\lim_{G\to\infty} p_{s_{CAP}} = 0$. When, instead, GTSs are allocated (Figure 9), there exists an horizontal asymptote, given by (by using eq. (25)):

$$\lim_{G\to\infty} S = \frac{z \cdot N_{GTS}}{T_A}\,. \tag{26}$$

As an example, when $SO = 1$ and $D = 10$, the maximum number of GTSs allocable is $N_{GTS} = 6$ and the horizontal asymptote is $S = 19531.25\ [bytes/sec]$.

B. The Tree-Based Topology

Numerical results obtained in the three-level tree are discussed here, and compared with results obtained in the star topology case. Since $p_{s_{tree}}$ and $D_{mean_{tree}}$ and $P\{Z^s\}$, depend on p_s obtained in the star topology case, that have been validated above, simulation results are not reported here.

In Figure 10 $p_{s_{tree}}$ as a function of N_1, for different values of N, D and SO, having set $BO = 5$, is shown. There exists an optimum value of N_1 maximising $p_{s_{tree}}$, and this value obviously increases by increasing N and is approximatively equal to $\sqrt{N}$, therefore it is independent on D and SO. This means that, once we fix N, there exists an optimum split between level 1 and level 2 nodes, maximising the success probability.

In Figure 11 results related to the two topologies, showing the success probability as a function of N, for different values of SO and BO by setting $D = 5$, are compared. For a fair comparison, the success probability is computed by fixing the same value of T_B, therefore by giving to nodes the same time to transmit the data to the coordinator. To this aim, we set $SO = BO$ for the star topology, and we compare the case "star" with $SO = BO = 1$ with the case "tree" with $BO = 1$ and $SO = 0$. Whereas the case "star" with $SO = BO > 1$ (note that the cases $SO = BO =$ 2,3, etc.. bring to the same p_s) are compared with the cases "tree" with $BO > 1$, whatever SO is. In the "tree" case N_1 is set to the optimum value maximising $p_{s_{tree}}$ obtained from Figure 10. As we can see, when $BO = 1$, the "star" is preferable, since in the "tree" only one router has a part of the superframe allocated, therefore, many packets of level 2 nodes are lost. For $BO > 1$, instead, the "tree" outperforms the "star". The difference between the "star" and the "tree",

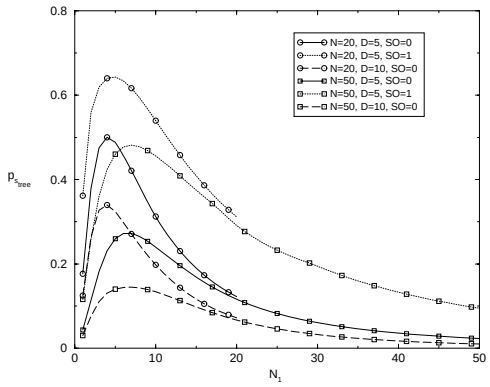

Fig. 10. The success probability, $p_{s_{tree}}$ as a function of N_1 for a tree-based topology.

obviously, increases by increasing BO and SO, resulting in an increase of p_{frame} and p_s, respectively.

In Fig. 12 the average delays obtained in case of star and tree-based topologies as a function of N, are shown. The curves are obtained by setting $D = 5$ and $N_1 = 3$ in the case of trees. The delays increase by increasing N, since the probability to find the channel busy and to delay the transmission gets larger. An horizontal asymptote is also present due to the maximum delay a packet may suffer, equal to the superframe duration, T_A, in the "star" case and to $T_B + T_A$ in the "tree" case. As expected the delays are larger for trees, since packets coming from level two nodes need two superframes to reach the coordinator. Also note that by increasing BO delays get significantly larger. The curves "tree" with $SO = 0$, $BO = 3$ and "tree" with $SO = 1$ and $BO = 3$ are overlapped since T_B assumes the same value and the delays of level one nodes are approximatively the same (in fact also the curves "star" with $SO = BO = 0$ and $SO = BO = 1$ are approximatively the same).

By comparing Figs. 11 and 12 we can, finally, deduce that the choice of the topology depends on the application requirements: in case the application requires large success probability, and it can tolerate large delays, trees are preferable; if, instead, more stringent constraints in terms of delays are imposed, star topologies are better. However note that trees allow to realise larger networks distributed in wide areas, whereas the number of nodes that may reach directly the coordinator is limited by connectivity problems. However the study of connectivity issues is out of the scope of this paper.

X. CONCLUSIONS

A mathematical model for the beacon-enabled mode of IEEE 802.15.4, is provided. The model captures all aspects of the standard air interface, and it allows the evaluation of the statistical distribution of the traffic generated by nodes toward the PAN coordinator, and of the probability that a node successfully transmits a packet. Results show how the distribution of the traffic, the throughput and the success probability change when different loads are offered. The model is validated through comparison with simulation results. A comparison between results obtained when star and tree-based topologies are considered, is also provided. Results show that,

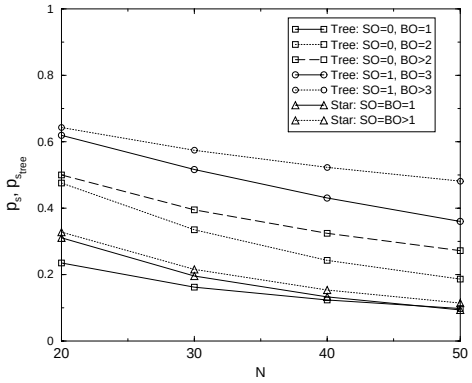

Fig. 11. The success probability as a function of N when a star and tree topologies are used.

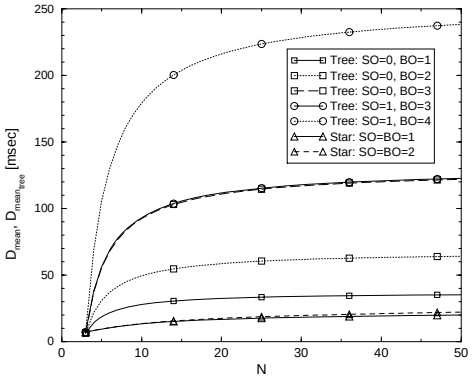

Fig. 12. The average delay as a function of N when a star and tree topologies are used.

in terms of success probability tree-based topologies are better in most of the cases, but bring to larger delays with respect to star topologies.

APPENDIX A
THE SENSING PROBABILITIES FOR $BO_s > 0$

We consider here the backoff stages $BO_s = 1, .., NB_{max}$ and we refer to the parts of the state transition diagram illustrated in Fig. 13 for the cases $W_{0,..,k-1} \leq W_k$ and in Fig. 14 for the cases $W_{0,..,k-1} > W_k$. Note that in the case of defaults MAC parameters ($BE_{min} = 3$, $BE_{max} = 5$ and $NB_{max} = 4$), Fig. 13 shows the cases $BO_s = 1$ and 2 and Fig. 14 the cases $BO_s = 3$ and 4.

As in the case $BO_s = 0$, the transition probabilities between backoff states in the k-th backoff stage, are given by:

$$P\{c, k, 2, j+1 | c+1, k, 2, j\} = 1 \,, \tag{27}$$

for $c \in [0, W_k - 2]$ and $j \in [k+2, W_{0,1,..,k} + k - 2]$, where $W_{0,1,..,k} = W_0 + W_1 + .. + W_k$. In the following we will denote as $W_{x,y,z}$ the sum $W_x + W_y + W_z$.

The transition probabilities between the sensing states at $CW = 2$ of the backoff stage k and those of the backoff stage $k+1$ are given by:

$$P\{c, k, 2, j+1 | 0, k-1, 2, j\} = \frac{b_2^j}{W_k} \,, \tag{28}$$

for $c \in [0, W_k - 1]$ and $j \in [k+1, W_{k-1} + k - 2]$. This equation accounts for the fact that in case a node is in the $k-1$-st backoff stage and the channel at slot j is found busy, the node will reach one of the states $\{c, k, 2, j+1\}$, with $c \in [0, W_k - 1]$, with the same probability $1/W_k$.

The transition probabilities between the sensing states of two subsequent backoff stages when $CW = 1$ are given by:

$$P\{c, k, 2, j+1 | 0, k-1, 1, j\} = \frac{b_1^j}{W_k} \,, \tag{29}$$

for $c \in [0, W_k - 1]$ and $j \in [k+1, W_{k-1} + k - 1]$.

If $W_{0,..,k-1} \leq W_k$ (see Fig. 13), the probabilities of being in sensing when $CW = 2$ are given by:

$$P\{S2_k^j\} = \begin{cases} \sum_{v=k+1}^{j-1} (P\{S1_{k-1}^v\} \cdot \frac{b_1^v}{W_k} + P\{S2_{k-1}^v\} \cdot \frac{b_2^v}{W_k}) \\ \qquad \text{for } j \in [k+2, W_{0,..,k-1} + k] \\ P\{S2_k^{W_{0,..,k-1}+k}\} \\ \qquad \text{for } j \in [W_{0,..,k-1} + k + 1, W_k + k + 1] \\ \sum_{v=j-W_k}^{W_{0,..,k-1}+k-1} (P\{S1_{k-1}^v\} \cdot \frac{b_1^v}{W_k} + P\{S2_{k-1}^v\} \cdot \\ \cdot \frac{b_2^v}{W_k}) \quad \text{for } j \in [W_k + k + 2, W_{0,..,k} + k - 1] \\ 0 \qquad \text{otherwise.} \end{cases} \tag{30}$$

Let us consider the case $BO_s = 1$, when $BE_{min} = 3$ and $BE_{max} = 5$. The first equation derives from the fact that until $j \leq W_0$, the probability of being in sensing in the second backoff stage depends on the probabilities of being in sensing in the first backoff stage and to find the channel busy the first or the second time. As an example, a node can arrive in $S2_1^3$ if it is in $S1_0^2$ or in $S2_0^2$, finds the channel busy, and extracts the value 0 for the second backoff stage (see Figs. 3 and 13). The second equation accounts for the fact that for $j > W_0 + 1$, there are no more transitions between the states of $BO_s = 0$ and the ones of $BO_s = 1$, because the last slot in which a node can sense the channel in the first backoff stage is $j = W_0 = 8$. Finally, when j reaches $W_1 + 3 = 19$, the sum starts with $v = 3$ and not 2, since if a node is in $S1_0^2$ (or in $S2_0^2$) it moves (in case of channel busy) to states $\{c, 1, 2, 3\}$ with $c \in [0, 15]$; therefore the state $\{16, 1, 2, 3\}$ does not exist (see the Figure).

Whereas, if $W_{0,..,k-1} > W_k$ (see Fig. 14), the probabilities of being in sensing when $CW = 2$ are given by:

$$P\{S2_k^j\} = \begin{cases} \sum_{v=k+1}^{j-1} (P\{S1_{k-1}^v\} \cdot \frac{b_1^v}{W_k} + P\{S2_{k-1}^v\} \cdot \frac{b_2^v}{W_2}) \\ \qquad \text{for } j \in [k+2, W_k + k + 1] \\ \sum_{v=j-W_k}^{j-1} (P\{S1_{k-1}^v\} \cdot \frac{b_1^v}{W_k} + P\{S2_{k-1}^v\} \cdot \frac{b_2^v}{W_k}) \\ \qquad \text{for } j \in [W_k + k + 2, W_{0,..,k-1} + k] \\ \sum_{v=j-W_k}^{W_{0,..,k-1}+k-1} (P\{S1_{k-1}^v\} \cdot \frac{b_1^v}{W_k} + \\ + P\{S2_{k-1}^v\} \cdot \frac{b_2^v}{W_k}) \\ \quad \text{for } j \in [W_{0,..,k-1} + k + 1, W_{0,..,k} + k - 1] \\ 0 \qquad \text{otherwise.} \end{cases} \tag{31}$$

Finally, the probabilities of being in sensing when $CW = 1$ when $BO_s = k$, with $k > 0$ are given by:

$$P\{S1_k^j\} = P\{S2_k^{j-1}\} \cdot (1 - b_2^{j-1}) \,, \tag{32}$$

for $j \in [k+3, W_{0,..,k} + k]$ and null otherwise.

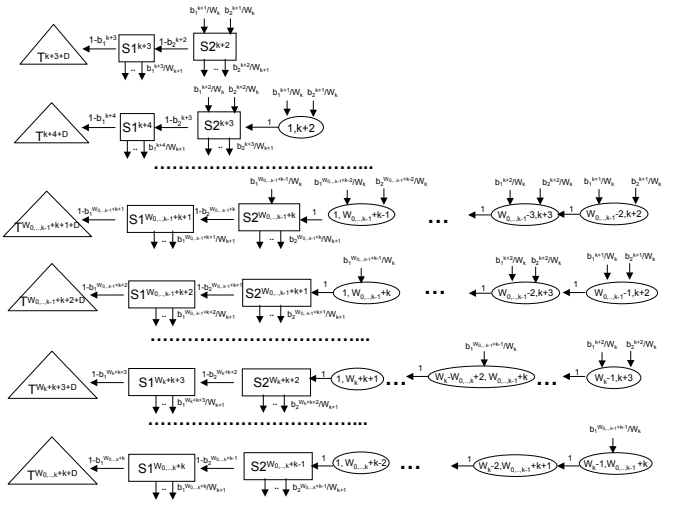

Fig. 13. The state-transition diagram of the k-th backoff stage, in the case $W_{0,..,k-1} \leq W_k$.

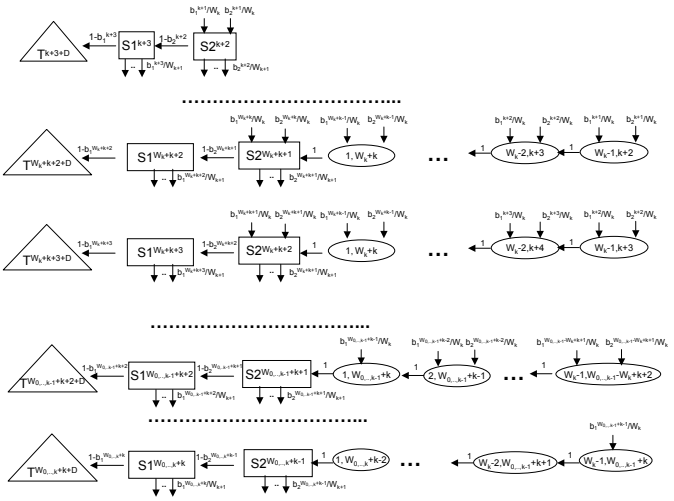

Fig. 14. The state-transition diagram of the k-th backoff stage, in the case $W_{0,..,k-1} > W_k$.

ACKNOWLEDGMENT

This work was supported by the European Commission in the framework of the FP7 Network of Excellence in Wireless COMmunications NEWCOM++ (contract n. 216715). The Author would also like to thank Roberto Verdone for the fruitful discussions on the model and on the paper results.

REFERENCES

[1] IEEE 802.15.4 Standard, *Part 15.4: Wireless Medium Access Control (MAC) and Physical Layer (PHY) Specifications for Low-Rate Wireless Personal Area Networks (LR-WPANs)*. Piscataway, New Jersey, 08855-1331: IEEE, 2006. [Online]. Available: http://standards.ieee.org/getieee802/802.15.html

[2] Z. Aliance, *Zigbee Specifications*. Zigbee Standard Organisation, 2008.

[3] E. Jovanov, "Wireless technology and system integration in body area networks for m-health applications," in *Proc. of 27th Annual International Conference on Engineering in Medicine and Biology Society, 2005*, 2005, pp. 7158–7160.

[4] R. Istepanian, E. Jovanov, and Y. Zhang, "Guest editorial introduction to the special section on m-health: Beyond seamless mobility and global wireless health-care connectivity," *IEEE Transactions on Information Technology in Biomedicine*, pp. 405–414, 2004.

[5] R. Verdone, D. Dardari, G. Mazzini, and A. Conti, *Wireless sensor and actuator networks*. Elsevier, 2008.

[6] I. F. Akyildiz, Y. S. Weilian Su, and E. Cayirci, "A survey on sensor networks," *IEEE Commun. Mag.*, vol. 40, no. 8, pp. 102–114, Aug. 2002.

[7] M. Tubaishat and S. Madria, "Sensor networks: an overview," *IEEE Potentials*, vol. 22, pp. 20–30, Apr. 2003.

[8] G. Lu, B. Krishnamachari, and C. S. Raghavendra, "Performance evaluation of the ieee 802.15.4 mac for low-rate low-power wireless networks," in *Workshop on Energy-Efficient Wireless Communications and Networks, 2004. EWCN 2004*, Apr. 2004, pp. 701–706.

[9] B. Bougard, F. Catthoor, D. C. Daly, A. Chandrakasan, and W. Dehaene, "Energy efficiency of the ieee 802.15.4 standard in dense wireless microsensor networks: Modeling and improvement perspectives," in *Proc. Design Automation and Test in Europe Conference and Exhibition, 2005*, Mar. 2005, pp. 196–201.

[10] M. Petrova, J. Riihijarvi, P. Mahonen, and S. Labella, "Performance study of ieee 802.15.4 using measurements and simulations," in *Proc. of IEEE WCNC 2006*, Apr. 2006, pp. 487–492.

[11] J. Misic, S. Shafi, and V. B. Misic, "Maintaining reliability through activity management in an 802.15.4 sensor cluster," *IEEE Trans. Veh. Technol.*, vol. 3, pp. 779–788, May 2006.

[12] S. Pollin, M. Ergen, S. Ergen, B. Bougard, L. V. der Pierre, F. Catthoor, I. Moerman, A. Bahai, and P. Varaiya, "Performance analysis of slotted carrier sense ieee 802.15.4 medium access layer," *IEEE Trans. Wireless Commun.*, vol. 7, pp. 3359–3371, Sept. 2008.

[13] G. Bianchi, "Performance analysis of the ieee 802.11 distributed coordination function," *IEEE J. Select. Areas Commun.*, vol. 18, pp. 535–547, Mar. 2000.

[14] C. Buratti and R. Verdone, "Performance analysis of ieee 802.15.4 non-beacon enabled mode," *To appear in IEEE Trans. on Vehicular Technologies*, 2009.

[15] T. Park, T. Kim, J. Choi, S. Choi, and W. Kwon, "Throughput and energy consumption analysis of ieee 802.15.4 slotted csma/ca," *IEEE Electronics Letters*, vol. 41, pp. 1017–1019, Sept. 2005.

[16] Z. Chen, C. Lin, H. Wen, and H. Yin, "An analytical model for evaluating ieee 802.15.4 csma/ca protocol in low rate wireless application," in *Proc. IEEE AINAW 2007*, 2007.

[17] I. Ramachandran, A. K. Das, and S. Roy, "Analysis of the contention access period of ieee 802.15.4 mac," *ACM Trans on Sensor Networks*, vol. 3, pp. 1–29, Mar. 2007.

[18] T. O. Kim, H. Kim, J. Lee, J. S. Park, and B. D. Choi, "Performance analysis of the ieee 802.15.4 with non beacon-enabled csma/ca in non-saturated contition," in *International Conference on Embedded And Ubiquitous Computing, 2006. EUC 2006*, Aug. 2006, pp. 884–893.

[19] J. Misic, V. B. Misic, and S. Shafi, "Performance of ieee 802.15.4 beacon-enabled pan with uplink transmissions in non-saturation mode - access delay for finite buffers," in *Proc. First International Conference on Broadband Networks, 2004. BroadNets 2004*, Oct. 2004, pp. 416–425.

[20] J. Misic, S. Shafi, and V. B. Misic, "The impact of mac parameters on the performance of 802.15.4 pan," *Elsevier Ad hoc Networks Journal*, vol. 3, pp. 509–528, Sept. 2005.

[21] C. Buratti and R. Verdone, "A mathematical model for performance analysis of ieee 802.15.4 non-beacon enabled mode," in *Proc. IEEE European Wireless, EW2008*, Prague, Czech Republic, June 2008.

[22] L. Kleinrock, *Queueing Systems*. John Wiley and Sons, 1975.

[23] A. Koubaa, M. Alves, and E. Tovar, "Modeling and worst-case dimensioning of cluster-tree wireless sensor networks," in *27th IEEE International Real-Time Systems Symposium, 2006, RTSS 2006*, Dec. 2006, pp. 412–421.